Osteogenic Differentiation of Adipose-Derived Stem Cells Is Hypoxia-Inducible Factor-1 Independent

Suchit Sahai, BS,[1] Amanda Williams,[1] Matthew L. Skiles, BS,[1] and James O. Blanchette, PhD[1,2]

Tissue engineering is a promising approach to repair critical-size defects in bone. Damage to vasculature at the defect site can create a lower O_2 environment compared with healthy bone. Local O_2 levels influence stem cell behavior, as O_2 is not only a nutrient, but also a signaling molecule. The hypoxia-inducible factor-1 (HIF-1) is a transcription factor that regulates a wide range of O_2-related genes and its contribution in bone repair/formation is an important area that can be exploited. In this study, we examined the effect of low O_2 environments (1% and 2% O_2) on the osteogenic differentiation of adipose-derived stem cells in both two-dimensional (2-D) and three-dimensional (3-D) culture systems. To determine the role of HIF-1 in the differentiation process, an inhibitor was used to block the HIF-1 activity. The samples were examined for osteogenesis markers as measured by quantification of the alkaline phosphatase (*ALP*) activity, mineral deposition, and expression of osteonectin (*ON*) and osteopontin (*OPN*). Results show a downregulation of the osteogenic markers (*ALP* activity, mineralization, *ON*, *OPN*) in both 1% and 2% O_2 when compared to 20% O_2 in both 2-D and 3-D culture. Vascular endothelial growth factor secretion over 28 days was significantly higher in low O_2 environments and HIF-1 inhibition reduced this effect. The inhibition of the HIF-1 activity did not have a significant impact on the expression of the osteogenic markers, suggesting HIF-1-independent inhibition of osteogenic differentiation in hypoxic conditions.

Introduction

CRITICAL-SIZE BONE DEFECTS (CSDs), which can result from trauma, infection, genetic abnormalities, and tumors, represent a challenge to the medical community. Tissue engineers seek to address this through implantation of cell-seeded scaffolds to fill these defects and accelerate formation of new bone.[1–4] Adipose-derived mesenchymal stem cells (ADSCs) represent a potential source of cells for these strategies as they are more easily harvested than bone marrow–derived mesenchymal stem cells and can differentiate into chondrocytes, osteoblasts, and vascular cell phenotypes.[5–7]

The loss of vasculature at CSD sites creates a hypoxic environment with O_2 concentrations of $\sim 0\%$–3%.[8–11] Hypoxia can exert a significant influence on stem cell behavior as O_2 is not only a nutrient, but a signaling molecule.[12–15] Hypoxia-inducible factor 1 (HIF-1) is a heterodimeric transcription factor. The stability of the alpha subunit (*HIF-1α*) is primarily regulated by the O_2 concentration. HIF-1 drives transcription of a wide range of O_2-regulated genes through interaction with hypoxia-responsive elements in their promoters, introns, and/or 3' enhancers.[16,17] Many stem cells are found in hypoxic environments in the body (defined as $< 5\%$ O_2) and the HIF activity is critical in embryonic development.[18–20] The important role HIF-1 plays in bone formation and repair has been discussed in a number of prior reviews.[21–23]

Formation of new, vascularized bone to repair a CSD is a complex process involving numerous cell types and interplay of biochemical, mechanical, and environmental stimuli. This contributes to the difficulty in interpreting results regarding the importance of hypoxia and HIF signaling in these processes. Studies conducted *in vivo* have shown the importance of HIF signaling on bone formation and repair, but it is difficult to decouple osteogenesis from angiogenesis.[24,25] Hypoxic signaling is a major driving force for angiogenesis and the vascular endothelial growth factor (*VEGF*) is a critical target of the HIF activity.[26,27] HIF-1 plays a key role in blood vessel formation and blocking the HIF-1 activity will impair vascular growth and bone repair.

The HIF-1 activity is also involved in chondrogenesis and maintenance of chondrocyte viability that are essential steps in endochondral bone formation.[28–30] The steps toward bone formation are difficult to track and isolate in *in vivo*, and while the HIF activity seems to be essential for bone formation in general, its impact on osteogenesis is less clear.

The majority of the literature indicates an inhibitory role for hypoxia on osteogenesis of mesenchymal stem cells *in vitro*.[31–36] A few studies, however, have shown the opposite effect.[37,38] This could be due to varied cell sources, a

[1]Biomedical Engineering Program, and [2]Department of Chemical Engineering, College of Engineering and Computing, University of South Carolina, Columbia, South Carolina.

range of O_2 conditions used to represent hypoxic conditions, and the timing of hypoxic exposure.[39]

Bone formation strategies taking place *ex vivo* can occur in a wide range of possible O_2 concentrations and many utilize atmospheric conditions (20% O_2). However, when differentiation takes place at a CSD, the environment will be hypoxic. Determination of whether *HIF-1α* represents a therapeutic target with respect to osteogenesis would enhance bone tissue-engineering efforts. Our studies were designed to provide information about the impact of hypoxia on osteogenesis of ADSCs in both two-dimensional (2-D) and three-dimensional (3-D) culture conditions and whether blocking the HIF-1 activity would alter this effect. *VEGF* secretion from ADSCs in identical conditions was also monitored as coupling of osteogenesis and angiogenesis is essential to recreate endochondral bone formation.

Materials and Methods

Cell culture

Human ADSCs were purchased from Invitrogen and cell culture was performed according to the supplier's specifications. Cells were cultured in the proprietary MesenPRO RS™ basal medium supplemented with the MesenPRO RS Growth Supplement, 1% penicillin/streptomycin (Mediatech), and 2 mM L-glutamine (MP Biomedicals). Culture conditions for passaging were maintained at 95% air and 5% CO_2 at 37°C. For experiments, cells between passages 2 and 7 were used as recommended by the supplier.

Hypoxic culture conditions

Nitrogen-purged, programmable incubators were used to maintain a constant 1% or 2% O_2 level for hypoxic studies (Napco Series 8000 WJ; Thermo Electron). For 1% or 2% O_2 experiments, all media, buffered salt solutions, and fixatives to be used with cells were kept in vented tubes in the hypoxic incubator for 24 h before use so as to equilibrate the solutions to the appropriate dissolved O_2 concentration. Previous studies in our laboratory have shown this period to be sufficient to equilibrate the dissolved O_2 concentration.[40] Media changes and imaging procedures were kept under 10 min per day to limit exposure to atmospheric conditions. Dissolved O_2 concentration studies conducted in our laboratory showed that levels rose from 0.3 to 0.4 mg/L during a 10-min atmospheric exposure (which correlates to a 1% O_2 to 1.5% O_2 environment). The 1% or 2% O_2 levels are re-established within 10 min of return to the incubator.

Cell encapsulation for 3-D experiments

Poly(ethylene glycol) (PEG) with an average molecular weight of 10,000 Da (Sigma-Aldrich) was functionalized by addition of methacrylate end groups resulting in poly(ethylene glycol) dimethacrylate (PEGDM) using a previously published method.[41] ADSCs were trypsinized, counted using a hemocytometer, and spun down in a microcentrifuge tube before removal of the media. Cells were then resuspended in a solution of 10 wt% PEGDM and 0.025 wt% 2-hydoxy-1-[4-(2-hydroxyethoxy)-phenyl]-2-methyl-1-propanone (Irgacure 2959; Ciba), which is a photoinitiator in the Hank's balanced salt solution (HBSS; Mediatech). ADSCs were suspended in

PEGDM to create a concentration of 10,000 cells/μL. For each gel, 40 μL of this ADSC/PEGDM suspension was added to a 1-mL syringe and exposed to a 365 nm light source at an intensity of 7 mW·cm^{-2} for 10 min under sterile conditions. The resulting gels were transferred to a 24-well plate, washed in HBSS, and placed in 1 mL of media. The plates were cultured in the varied O_2 conditions on orbital shakers set to continuous rotation at 100 rpm. The encapsulation process is shown in a previously published video.[42]

Osteogenic differentiation

Osteogenic differentiation was induced by culture in the StemPro® Osteocyte/Chondrocyte Differentiation Basal Medium and StemPro Osteogenesis Supplement (Invitrogen). These experiments were carried out for ADSCs in 2-D (100,000 ADSCs seeded per well of 12-well culture plates) as well as 3-D environments (encapsulated ADSCs as detailed in the previous section). The cells were monitored over a period of 28 days in 1%, 2%, and 20% O_2 with the osteogenic medium replenished every 3 days.

HIF-1 inhibition

To inhibit the activity of HIF-1, a HIF-1 inhibitor {3-[2-(4-adamantan-1-yl-phenoxy)-acetylamino]-4-hydroxybenzoic acid methyl ester; Calbiochem} was used. It is a cell-permeable amidophenolic compound that inhibits the hypoxia-induced HIF-1 transcription activity. The inhibitor selectively blocks the hypoxia-induced accumulation of the cellular *HIF-1α* protein, while exhibiting no apparent effect on the cellular level of *HIF-1α* mRNA or that of the *HIF-1β* protein. For both 1% and 2% O_2 samples, a concentration of 60 μM of this inhibitor was sufficient to reduce accumulation of HIF-1α to levels below detection in Western blotting (Supplementary Fig. S1; Supplementary Data are available online at www.liebertpub.com/tea). Toxicity tests showed no loss of viability of ADSCs exposed to the inhibitor at concentrations up to 100 μM (data not shown).

Alkaline phosphatase activity and DNA quantification

Measurements of the alkaline phosphatase (ALP) activity in the media of ADSCs were taken on days 7, 14, 21, and 28. The activity was determined using an ALP colorimetric assay kit (Abcam) with p-nitrophenyl phosphate as a substrate. The *ALP* activities were normalized to the cellular DNA content using a PicoGreen dsDNA quantitation kit (Molecular Probes) according to the manufacturer's instructions. The *ALP* activity is quantified on days 7, 14, 21, and 28 and is expressed in μmol/mL/min/mg DNA. The values included represent the mean of three independent studies.

Alizarin Red staining for mineralization

Mineral deposition was quantified on days 14 and 28 using the Alizarin Red S staining procedure. The cells were rinsed with calcium- and phosphate-free HBSS, and fixed with ice-cold 70% ethanol for 1 h. After a brief wash with HBSS, the cells were stained for 20 min with 40 mM of the Alizarin Red solution (pH 4.2) at room temperature (RT). The cells were rinsed two times for 15 min with HBSS (on an orbital shaker) to reduce nonspecific Alizarin Red staining. A

10% acetic acid was then added to the samples for 30 min on a shaker. Samples were collected by scraping (2-D) or vortex (3-D) and heated at 80°C for 10 min. The extracts are then centrifuged at 8000 rpm for 20 min and quantified spectrophotometrically with a microplate reader (Biotek) at 570 nm. The calcium concentration was calculated from the standard curve generated from a serial dilution of a calcium standard solution, and the values were normalized to DNA contents (expressed in mg mineral/mg DNA). Values included represent the mean of three independent studies.

Protein expression

Total cell lysates were collected from the 2-D and 3-D samples with the radio immunoprecipitation assay (RIPA) lysis buffer containing a protease and phosphatase inhibitor cocktail (Thermo Scientific), stirred on ice for 10 min, and sonicated for 15 min. The mixtures were then centrifuged at 14,000 rpm at 4°C for 15 min. The supernatants were collected and the protein concentration was quantified using a Coomassie Plus Bradford Assay kit (Thermo Scientific) according to the manufacturers' instructions.

Western blotting was performed by sodium dodecyl sulfate polyacrylamide gel electrophoresis (SDS-PAGE) with 50 µg of protein lysate loaded per lane of 4%–20% gradient gels followed by transfer to polyvinylidene fluoride membranes (Millipore). The membrane was first incubated in 5% dry milk, 1% bovine serum albumin (BSA) diluted in HBSS for 1 h at RT. The membrane was then washed twice for 10 min each in wash 1 (0.1% Tween-20, 0.1% dry milk, 0.1% BSA in HBSS). The membrane was then incubated with rabbit anti-*HIF-1α* antibody (1:1000; Santa Cruz Biotechnology), rabbit anti-osteonectin/*SPARC* antibody (1:1000), anti-osteopontin (*OPN*; 1:1000), or rabbit anti-β-actin antibody (1:1000; Santa Cruz Biotechnology) for 2 h at RT. The membrane was then washed three times for 10 min each in wash 1. Membranes were then incubated with peroxidase-conjugated goat anti-rabbit IgG (1:5000; Rockland Immunochemicals) for 2 h at RT. Membranes were then washed three times for 10 min each in wash 2 (0.1% Tween-20 in HBSS). Protein detection was achieved by a 5-min incubation in a chemiluminescence reagent, SuperSignal West Pico Substrate (Thermo Scientific). Bands were then detected using ChemiDoc™ XRS$^+$ System with Image Lab™ image acquisition and analysis software (Bio-Rad). With densitometry analysis, the expression of proteins was normalized to β-actin and multiplied by 100 to generate a % intensity optical density (IOD) fold difference of protein expression. All incubation steps and washes were performed on an orbital shaker set to continuous rotation at 100 rpm. The statistics shown represent results obtained from three independent studies.

VEGF release

VEGF release was monitored in 2-D and 3-D samples with and without the HIF-1 inhibitor over 28 days. The supernatant was collected on days 1, 4, 7, and 28 and *VEGF* levels were determined using a colorimetric *VEGF* enzyme-linked immuno sorbent assay (ELISA) kit according to the manufacturer's instructions (Invitrogen). The absorbance was measured at 450 nm and *VEGF* standards are used to calculate a VEGF concentration. These values are multiplied by the volume used during the release studies, normalized relative to the viable cell number and expressed as (fg/cell). The data represent three independent studies and release over a 24-h period for all time points.

Viability of ADSCs

A Live/Dead® staining kit (Invitrogen) was used to test the viability of the samples over 28 days. Fluorescent dyes indicate an esterase activity (observed as the green signal in live cells) or a loss of nuclear membrane integrity (observed as the red signal in dead cells). The 2-D and 3-D samples were kept in culture conditions identical to the previous experiments and the staining was performed in accordance with the manufacturer's guidelines. Results are given as a percentage of viable cells based on analysis of three independent studies.

Statistical analysis

Statistical analysis was performed using Graphpad Prism 4.01 (GraphPad Software Inc.). Experimental results are expressed as the mean ± standard deviation. All the collected data were analyzed by two-way analysis of variance (ANOVA) for comparisons and p-values <0.05 were defined as statistically significant differences.

Results

ALP activity

In 2-D, the *ALP* activity at 20% O_2 without the HIF inhibitor was 9.15±0.93, 22.11±3.14, 32.01±3.14, and 33.98±2.34 µmol/mL/min/mg DNA on days 7, 14, 21, and 28, respectively. With the HIF inhibitor, the *ALP* levels were 8.43±2.76, 20.21±2.47, 28.73±2.31, and 31.79±3.12 µmol/mL/min/mg DNA on days 7, 14, 21, and 28, respectively. At 2% O_2, the *ALP* levels without the inhibitor were 9.42±0.72, 20.35±3.31, 21.82±3.32, and 23.21±1.68 µmol/mL/min/mg DNA on days 7, 14, 21, and 28, respectively. With the inhibitor, the *ALP* levels were 6.45±1.43, 18.75±2.36, 22.36±1.92, and 24.42±2.67 µmol/mL/min/mg DNA on days 7, 14, 21, and 28, respectively. At 1% O_2, *ALP* levels without the inhibitor were 8.11±0.91, 19.43±1.87, 23.13±1.21, and 23.89±1.62 µmol/mL/min/mg DNA on days 7, 14, 21, and 28, respectively. With the HIF inhibitor, the *ALP* levels were 10.1±1.32, 16.23±2.42, 19.87±1.91, and 21.42±2.63 µmol/mL/min/mg DNA. These results are shown in Figure 1A.

In 3-D, *ALP* levels at 20% O_2 without the HIF inhibitor were 7.75±0.76, 19.11±1.34, 28.17±2.53, and 35.39±3.25 µmol/mL/min/mg DNA on days 7, 14, 21, and 28, respectively. With the inhibitor, the *ALP* levels were 8.91±1.65, 21.45±2.41, 27.81±3.11, and 38.21±3.22 µmol/mL/min/mg DNA on days 7, 14, 21, and 28, respectively. At 2% O_2, the *ALP* levels without the inhibitor were 7.51±0.75, 20.73±1.45, 23.26±3.62, and 24.32±2.33 µmol/mL/min/mg DNA on days 7, 14, 21, and 28, respectively. With the inhibitor, the *ALP* levels were 8.13±1.23, 17.53±2.62, 22.81±2.14, and 22.87±4.54 µmol/mL/min/mg DNA on days 7, 14, 21, and 28, respectively. At 1% O_2, the *ALP* levels without the inhibitor were 6.22±0.87, 16.95±1.52, 23.42±1.89, and 23.84±1.28 µmol/mL/min/mg DNA on days 7, 14, 21, and 28, respectively. With the inhibitor, the *ALP* levels were 9.65±1.54, 17.57±2.34, 21.42±3.73, and 22.13±2.51 µmol/mL/min/mg DNA on days 7, 14, 21, and 28, respectively. These results are shown in Figure 1B.
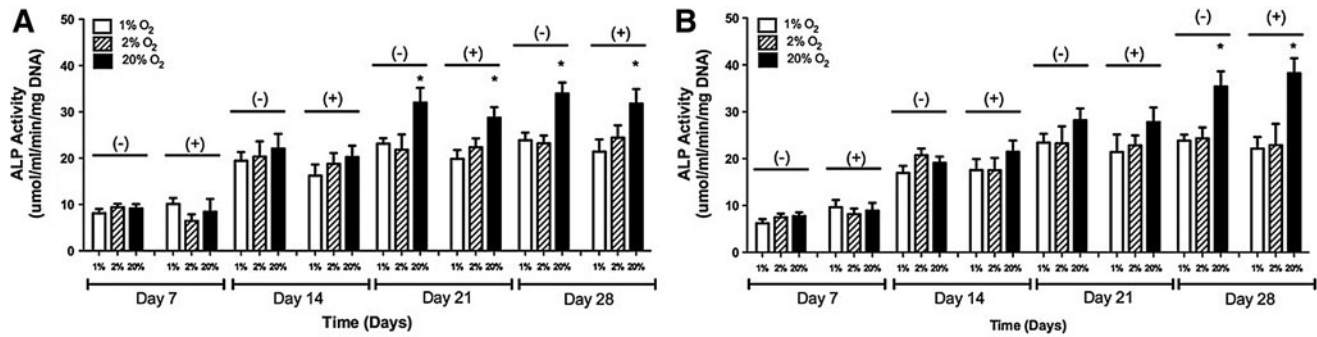
FIG. 1. The alkaline phosphatase (ALP) activity of adipose-derived, mesenchymal stem cells at 1%, 2%, and 20% O_2 with and without the hypoxia-inducible factor-1 inhibitor in **(A)** two-dimensional (2-D) and **(B)** three-dimensional (3-D) culture conditions over a period of 4 weeks. The values have been normalized by total DNA and represent the mean ± standard deviation. Statistically significant difference ($p < 0.05$) is marked by (*) indicating a higher activity at 20% O_2 in comparison to both 1% and 2% O_2.

Mineralization

In 2-D, at 20% O_2 and without the inhibitor, mineral deposition was observed to be 33.04 ± 1.61 and 55.28 ± 3.66 mg mineral/mg DNA on days 14 and 28, respectively. With the inhibitor, the mineral deposition levels were 31.13 ± 1.52 and 54.21 ± 3.54 mg mineral/mg DNA on days 14 and 28, respectively. At 2% O_2, the mineral deposition levels without the inhibitor were 11.34 ± 1.34 and 34.87 ± 2.76 mg mineral/ mg DNA on days 14 and 28, respectively. With the HIF inhibitor, the mineral deposition levels were 9.83 ± 3.16 and 32.45 ± 2.710 mg mineral/mg DNA on days 14 and 28, respectively. At 1% O_2, the mineral deposition levels without the inhibitor were 8.85 ± 0.63 and 32.04 ± 2.04 mg mineral/mg DNA on days 14 and 28, respectively. Without the inhibitor, the mineral deposition levels were 12.26 ± 2.17 and 31.52 ± 2.64 mg mineral/mg DNA on days 14 and 28, respectively. These results are shown in Figure 2A.

In 3-D samples, at 20% O_2 and without the inhibitor, mineral deposition was observed to be 32.07 ± 2.86 and 68.55 ± 3.19 mg mineral/mg DNA on days 14 and 28. With the inhibitor, the mineral deposition levels were 35.15 ± 3.23 and 65.42 ± 4.16 mg mineral/mg DNA on days 14 and 28, respectively. At 2% O_2, mineral deposition levels without the inhibitor were 28.56 ± 3.72 and 54.23 ± 4.28 mg mineral/mg

DNA on days 14 and 28, respectively. With the inhibitor, the mineral deposition levels were 30.24 ± 2.23 and 51.92 ± 3.54 mg mineral/mg DNA on days 14 and 28, respectively. At 1% O_2, mineral deposition levels without the inhibitor were 33.04 ± 1.52 and 51.77 ± 1.36 mg mineral/mg DNA on days 14 and 28. With the inhibitor, the mineral deposition levels were 35.71 ± 1.72 and 48.98 ± 3.41 mg mineral/mg DNA on days 14 and 28, respectively. These results are shown in Figure 2B.

HIF-1α protein expression

No *HIF-1α* protein was observed in 2-D studies when the inhibitor was present. In the absence of the inhibitor, no *HIF-1α* was observed at 20% O_2. In the absence of the inhibitor, *HIF-1α* expression of 6.31 ± 2.03 and 6.63 ± 2.32 %IOD fold difference was observed in 2% and 1% O_2 environments, respectively. A representative image of a gel and the collective results are shown in Figure 3A and B.

No *HIF-1α* protein was observed in 3-D studies when the inhibitor was present. In the absence of the inhibitor, *HIF-1α* expression of 1.14 ± 0.34, 5.12 ± 1.63, and 6.47 ± 1.91 %IOD fold difference was observed in 20%, 2%, and 1% O_2 environments, respectively. A representative image of a gel and the collective results are shown in Figure 4A and B.
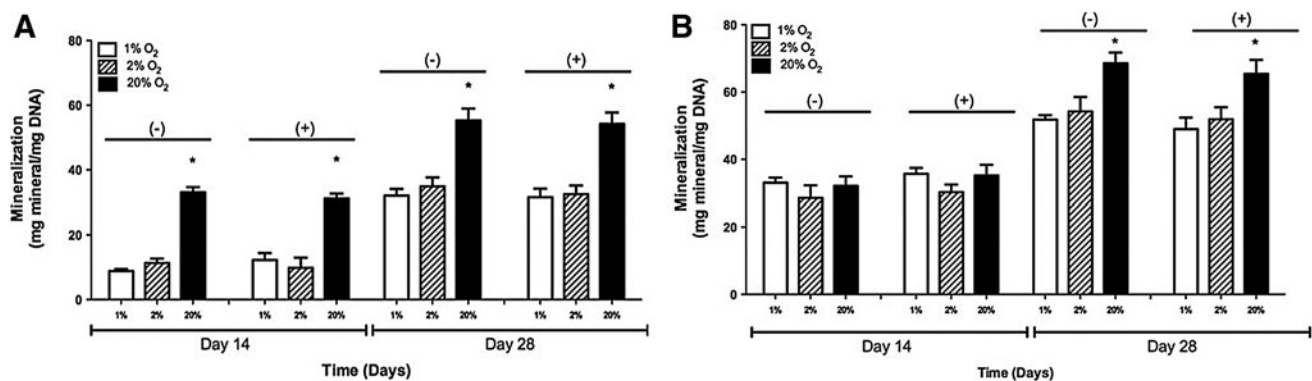

FIG. 2. Quantification of Alizarin Red staining of adipose-derived, mesenchymal stem cells cultured in 1%, 2%, and 20% O_2 with and without the hypoxia-inducible factor-1 inhibitor in **(A)** 2-D and **(B)** 3-D culture condition. The values have been normalized by total DNA and represent the mean ± standard deviation. Statistically significant difference ($p < 0.05$) is marked by (*) indicating higher absorbance at 20% O_2 in comparison to 1% and 2% O_2.
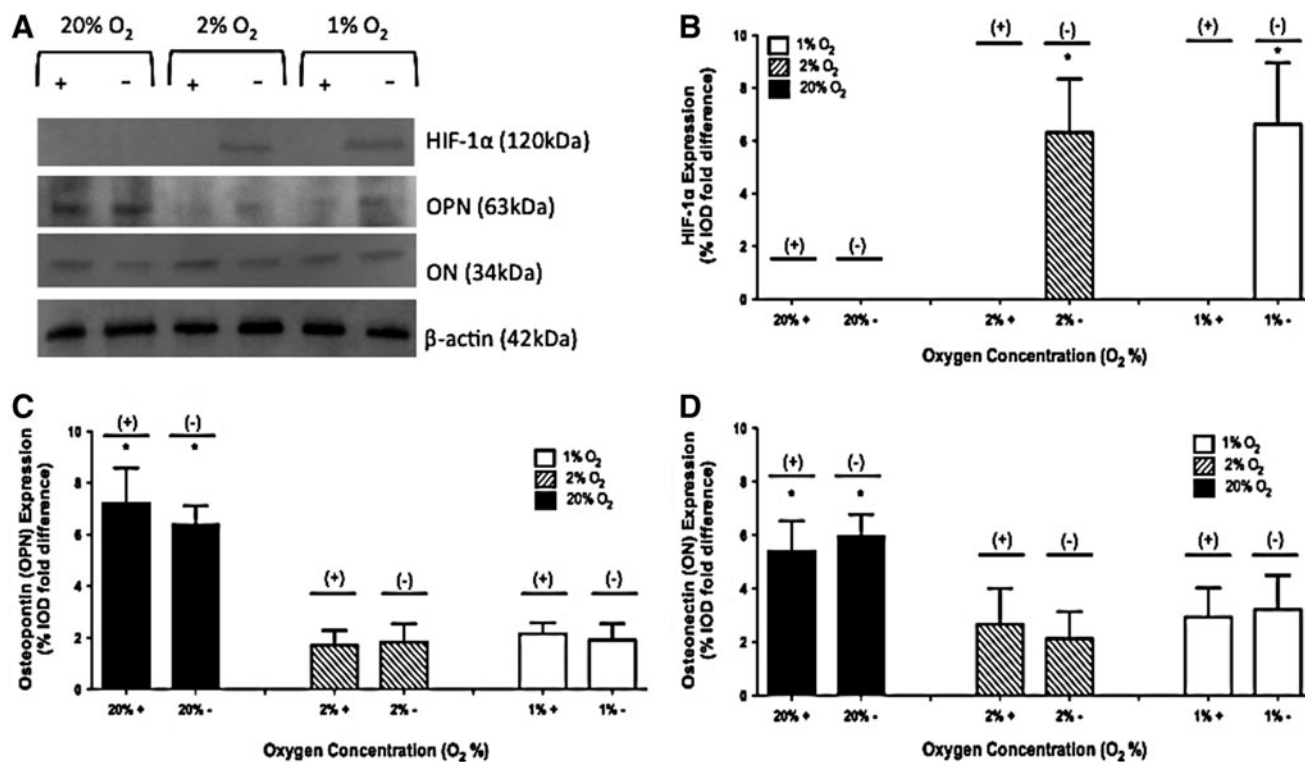
FIG. 3. Protein expression of hypoxia-inducible factor-1α (HIF-1α), osteopontin (OPN), and osteonectin (ON) on day 28 at 1%, 2%, and 20% O_2 with and without the HIF-1 inhibitor in 2-D culture. A representative gel is shown in **(A)**. Results of three independent studies are quantified in **(B)** HIF-1α, **(C)** OPN, and **(D)** ON. The values have been normalized to β-actin and represent the mean ± standard deviation. When a statistically significant difference ($p < 0.05$) is observed between 20% O_2 in comparison to 1% and 2% O_2, it is marked (*).

OPN protein expression

For 2-D studies in the absence of the inhibitor, *OPN* expression of 6.38 ± 0.73, 1.82 ± 0.72, and 1.92 ± 0.61 %IOD fold difference was observed in 20%, 2%, and 1% O_2 environments, respectively. When the inhibitor was present, *OPN* expression of 7.21 ± 1.37, 1.71 ± 0.57, and 2.15 ± 0.43 %IOD fold difference was observed in 20%, 2%, and 1% O_2 environments, respectively. A representative image of a gel and the collective results are shown in Figure 3A and C.

For 3-D studies in the absence of the inhibitor, *OPN* expression of 8.16 ± 1.12, 2.15 ± 0.83, and 1.79 ± 0.82 %IOD fold difference was observed in 20%, 2%, and 1% O_2 environments, respectively. When the inhibitor was present, *OPN* expression of 9.34 ± 0.54, 1.43 ± 0.61, and 1.23 ± 0.25 %IOD fold difference was observed in 20%, 2%, and 1% O_2 environments, respectively. A representative image of a gel and the collective results are shown in Figure 4A and C.

Osteonectin protein expression

For 2-D studies in the absence of the inhibitor, osteonectin (*ON*) expression of 5.97 ± 0.81, 2.13 ± 1.01, and 3.23 ± 1.27 %IOD fold difference was observed in 20%, 2%, and 1% O_2 environments, respectively. When the inhibitor was present, *ON* expression of 5.41 ± 1.13, 2.67 ± 1.34, and 2.93 ± 1.09 %IOD fold difference was observed in 20%, 2%, and 1% O_2 environments, respectively. A representative image of a gel and the collective results are shown in Figure 3A and D.

For 3-D studies in the absence of the inhibitor, *ON* expression of 6.88 ± 0.34, 2.33 ± 1.03, and 3.41 ± 1.65 %IOD fold difference was observed in 20%, 2%, and 1% O_2 environments, respectively. When the inhibitor was present, *ON* expression of 7.21 ± 0.87, 3.67 ± 1.24, and 2.45 ± 1.19 %IOD fold difference was observed in 20%, 2%, and 1% O_2 environments, respectively. A representative image of a gel and the collective results are shown in Figure 4A and D.

VEGF release

For 2-D studies at 20% O_2 in the absence of the inhibitor, *VEGF* secretion was 1.52 ± 0.21, 1.39 ± 0.12, 1.63 ± 0.16, and 1.78 ± 0.23 fg/cell on days 1, 4, 7, and 28, respectively. With the HIF inhibitor, *VEGF* secretion was 1.81 ± 0.55, 1.09 ± 0.30, 1.61 ± 0.25, and 2.08 ± 0.15 fg/cell on days 1, 4, 7, and 28, respectively. At 2% O_2 in the absence of the inhibitor, *VEGF* secretion was 23.51 ± 2.13, 15.07 ± 1.29, 12.82 ± 0.84, and 5.21 ± 0.94 fg/cell on days 1, 4, 7, and 28, respectively. With the HIF inhibitor, *VEGF* secretion was 4.51 ± 1.38, 1.77 ± 0.28, 1.64 ± 0.08, and 1.88 ± 0.30 fg/cell on days 1, 4, 7, and 28, respectively. At 1% O_2 in the absence of the inhibitor, *VEGF* secretion was 31.26 ± 1.24, 15.14 ± 1.13, 12.55 ± 0.92, and 7.57 ± 0.48 fg/cell on days 1, 4, 7, and 28, respectively. With the HIF inhibitor, *VEGF* secretion was 5.78 ± 0.82, 2.30 ± 0.31, 2.48 ± 0.47, and 1.67 ± 0.25 fg/cell on days 1, 4, 7, and 28, respectively. The VEGF release results for 2-D studies are shown in Figure 5A.

For 3-D studies at 20% O_2 in the absence of the inhibitor, *VEGF* secretion was 0.80 ± 0.33, 0.40 ± 0.23, 0.41 ± 0.10, and
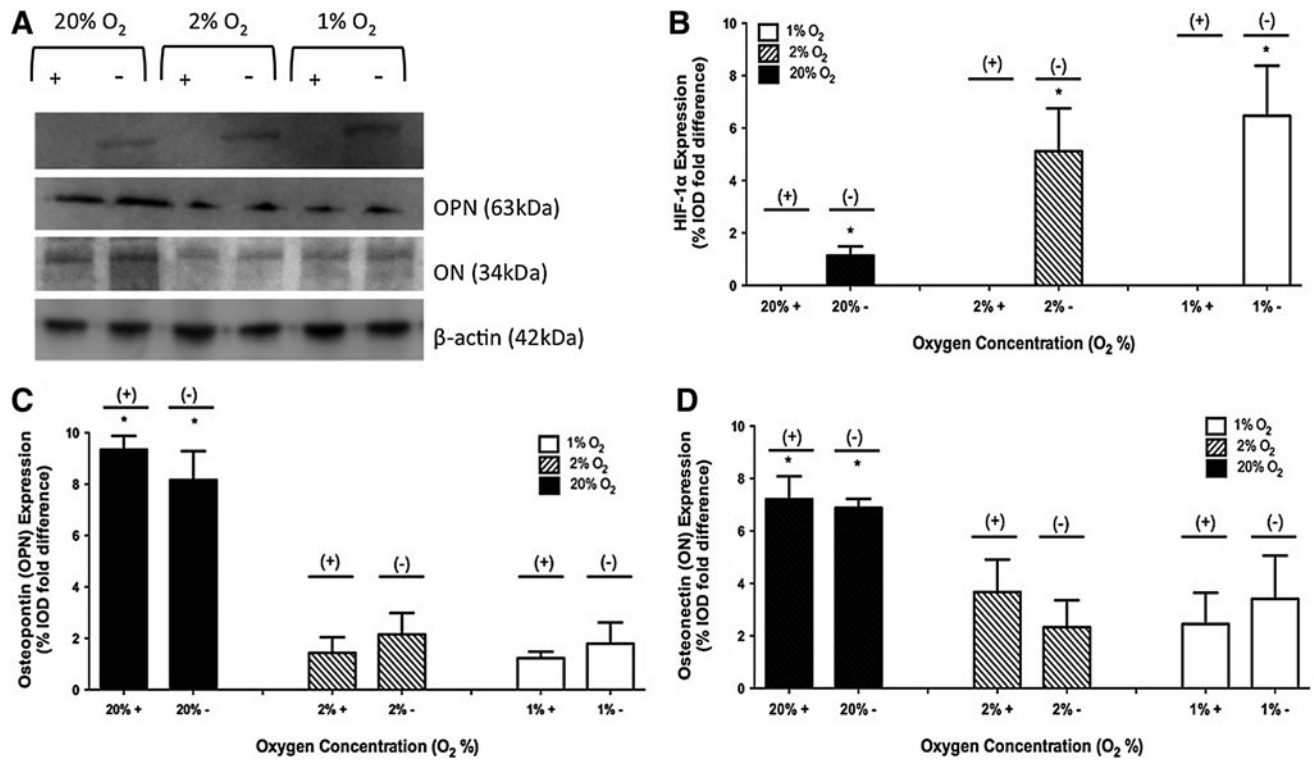
FIG. 4. Protein expression of HIF-1α, OPN, and ON on day 28 at 1%, 2%, and 20% O_2 with and without the HIF-1 inhibitor in 3-D culture. A representative gel is shown in **(A)**. Results of three independent studies are quantified in **(B)** HIF-1α, **(C)** OPN, and **(D)** ON. The values have been normalized to β-actin and represent the mean±standard deviation. When a statistically significant difference ($p < 0.05$) is observed between 20% O_2 in comparison to 1% and 2% O_2, it is marked (*).

0.51±0.22 fg/cell on days 1, 4, 7, and 28, respectively. With the HIF inhibitor, *VEGF* secretion was 1.2±0.18, 0.68±0.10, 0.60±0.08, and 0.54±0.12 fg/cell on days 1, 4, 7, and 28, respectively. At 2% O_2 in the absence of the inhibitor, *VEGF* secretion was 14.86±0.71, 6.91±0.46, 7.18±0.36, and 4.82±0.23 fg/cell on days 1, 4, 7, and 28, respectively.

With the HIF inhibitor, *VEGF* secretion was 1.61±0.11, 0.74±0.065, 0.61±0.23, and 1.19±0.06 fg/cell on days 1, 4, 7, and 28, respectively. At 1% O_2 in the absence of the inhibitor, *VEGF* secretion was 15.43±0.41, 8.32±0.26, 7.00±0.41, and 4.42±0.28 fg/cell on days 1, 4, 7, and 28, respectively. With the HIF inhibitor, *VEGF* secretion was 1.80±0.15,
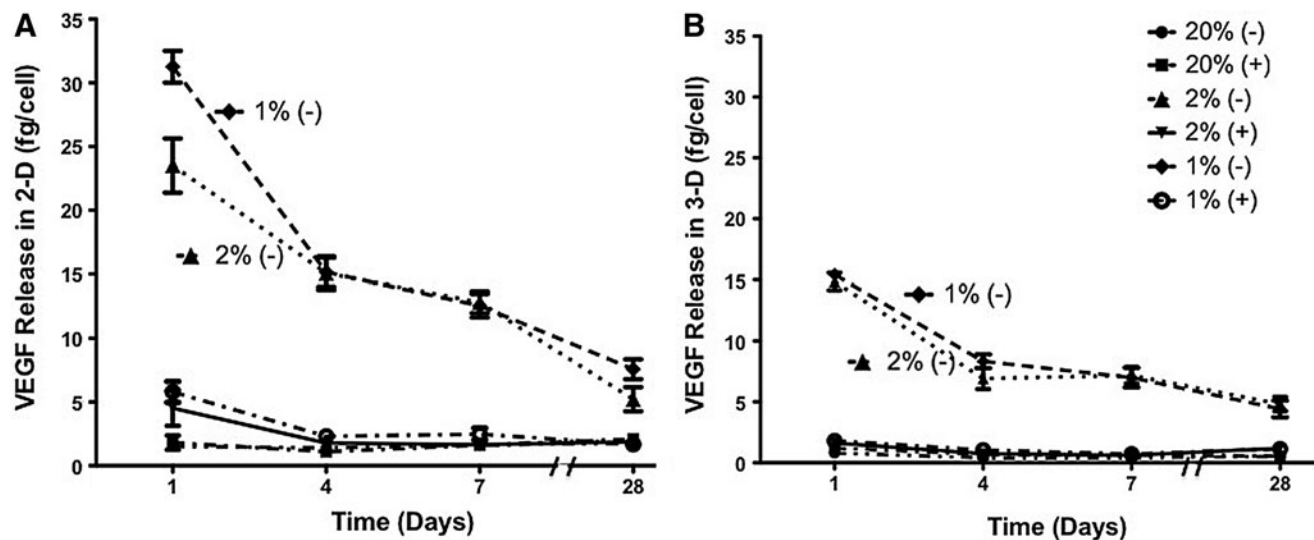

FIG. 5. Vascular endothelial growth factor (VEGF) release of adipose-derived, mesenchymal stem cells at 1%, 2%, and 20% O_2 with and without the HIF-1 inhibitor in **(A)** 2-D and **(B)** 3-D culture conditions over a period of 4 weeks. The values have been normalized by a viable cell number and represent the mean±standard deviation.
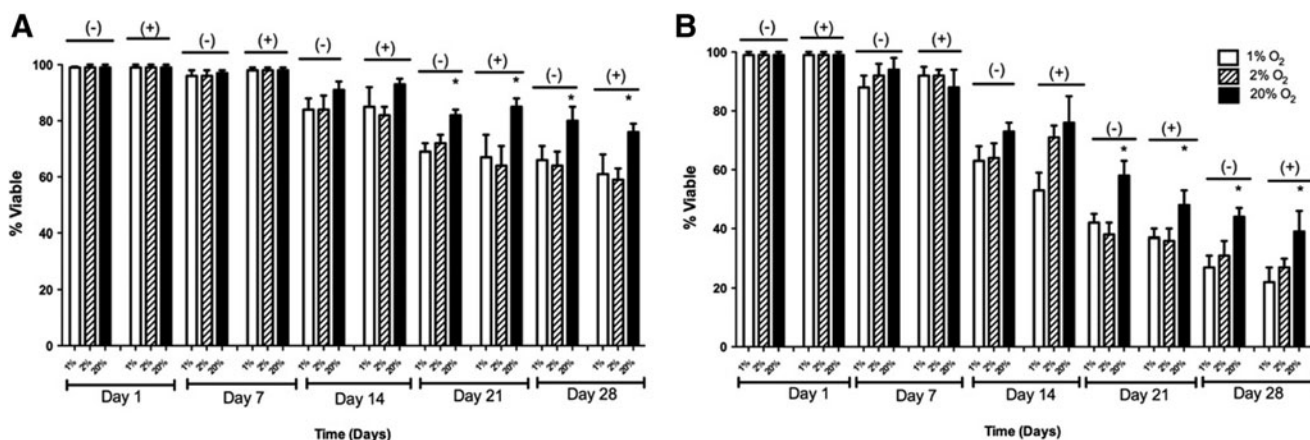
FIG. 6. Viability of adipose-derived, mesenchymal stem cells in 1%, 2%, and 20% O_2 with and without the HIF-1 inhibitor in **(A)** 2-D and **(B)** 3-D culture conditions over a period of 4 weeks. The values shown represent the mean ± standard deviation from three independent experiments. When a statistically significant difference ($p < 0.05$) is observed between 20% O_2 in comparison to 1% and 2% O_2, it is marked (*) for both 2-D and 3-D studies.

1.04 ± 0.16, 0.71 ± 0.08, and 1.13 ± 0.20 fg/cell on days 1, 4, 7, and 28, respectively. The VEGF release results for 3-D studies are shown in Figure 5B.

ADSC viability

In 2-D, at 20% O_2 and without the inhibitor, the percent viability was 99% ± 1%, 97% ± 1%, 91% ± 2%, 84% ± 4%, and 81% ± 6% on days 1, 7, 14, 21, and 28, respectively. With the HIF inhibitor, the percent viability was 99% ± 1%, 98% ± 1%, 93% ± 2%, 85% ± 6%, and 78% ± 4% on days 1, 7, 14, and 28, respectively. At 2% O_2, the percent viability without the inhibitor were 99% ± 1%, 96% ± 2%, 84% ± 5%, 72% ± 3%, and 64% ± 5% on days 1, 7, 14, 21, and 28, respectively. With the inhibitor, the percent viability was 99% ± 1%, 98% ± 1%, 82% ± 3%, 64% ± 7%, and 59% ± 5% with the inhibitor on days 1, 7, 14, 21, and 28, respectively. At 1% O_2, percent viability with the inhibitor was 99% ± 1%, 96% ± 2%, 84% ± 3%, 69% ± 4%, and 66% ± 4% on days 1, 7, 14, 21, and 28, respectively. With the inhibitor, the percent viability was 99% ± 1%, 98% ± 1%, 85% ± 7%, 73% ± 5%, and 61% ± 7% on days 1, 7, 14, 21, and 28, respectively. These results are shown in Figure 6A.

In 3-D culture, at 20% O_2 and without the inhibitor, percent viability was 99% ± 1%, 94% ± 4%, 75% ± 4%, 61% ± 4%, and 47% ± 6% on days 1, 7, 14, 21, and 28, respectively. With the HIF inhibitor, the percent viability was 99% ± 1%, 89% ± 6%, 76% ± 7%, 58% ± 6%, and 44% ± 3% on days 1, 7, 14, 21, and 28, respectively. At 2% O_2, percent viability without the inhibitor was 99% ± 1%, 92% ± 4%, 66% ± 5%, 46% ± 3%, and 33% ± 5% on days 1, 7, 14, 21, and 28, respectively. With the inhibitor, the percent viability was 99% ± 1%, 89% ± 3%, 71% ± 4%, 43% ± 7%, and 36% ± 6% with the inhibitor on days 1, 7, 14, 21, and 28, respectively. At 1% O_2, percent viability without the inhibitor was 99% ± 1%, 88% ± 5%, 63% ± 6%, 42% ± 3%, and 29% ± 5% on days 1, 7, 14, 21, and 28, respectively. With the inhibitor, the percent viability was 99% ± 1%, 92% ± 3%, 55% ± 4%, 38% ± 6%, and 27% ± 3% on days 1, 7, 14, 21, and 28, respectively. These results are shown in Figure 6B.

Discussion

Our results demonstrate a reduced capacity for ADSCs to differentiate into osteoblasts in hypoxic conditions when compared with atmospheric conditions. ADSCs in 1% and 2% O_2 environments displayed a reduced ALP activity, mineralization, and expression of *ON* and *OPN* in 2-D and 3-D culture geometries compared with ADSCs in 20% O_2 environments. The HIF-1 activity does not appear to be an essential component of the varied response of ADSCs in hypoxic conditions. For all O_2 concentrations and in both 2-D and 3-D cultures, pharmacologically induced inhibition of *HIF-1α* had no impact on any of these markers of osteogenesis.

Viability of ADSCs dropped over the course of our differentiation experiment, but our data are normalized to total DNA or β-actin to account for this. The viability decrease in 3-D was more pronounced than for 2-D cultures and this was probably a result of using an unmodified PEG gel. Previous work has shown that integrating integrin-binding sequences into the scaffold or genetic modification of cells can extend survival of mesenchymal stem cells (MSCs) in these materials by preventing anoikis.[43] We utilized a blank PEG gel to remove the impact of peptide modification on osteogenic differentiation, but future studies could evaluate peptide-modified PEG gels in combination with varied O_2 concentrations.

As mentioned earlier, the literature shows mixed results concerning the impact of hypoxic conditions on osteogenesis and healing of CSDs. Given the large number of variables in play, this is not surprising. Different research groups utilize a range of cell types and hypoxic conditions vary across the entire range from below 1% up to 5% O_2. When 3-D studies are conducted, O_2 levels and the state of hypoxic signaling can vary widely for cells depending on experimental conditions (size of scaffolds, scaffold material(s), and cell density within scaffolds, for example). All of these factors make it difficult to draw definitive conclusions regarding the impact of hypoxia on bone formation that will hold regardless of the cell type employed and O_2 concentration used.

Previous studies that have examined the role of HIF-1 through genetic engineering, have demonstrated how changes in the experimental procedure can impact the results. Three factors stand out in addition to those mentioned above. First, the role of HIF-1 may be impacted by whether the studies are investigating intramembranous or endochondral bone formation. Our studies are an *in vitro* model of intramembranous bone formation as mesenchymal stem cells are directly differentiated into osteoblasts. Our results are in agreement with a previous study that showed no impact on *HIF-1α* deletion on osteogenic differentiation of ADSCs.[29] Mice lacking *HIF-1α* showed impaired formation of long bones (endochondral), but no impact on bone formation in the skull (intramembranous).[24] The HIF-1 activity has been linked to chondrogenesis so whether this step is necessary could explain the varied results.[30,44]

Second, the HIF-1 activity has also been shown to impact angiogenesis.[22,23] Our *in vitro* work included studies to look at *VEGF* release, which correlated with the O_2 concentrations. Inhibition of HIF-1 also inhibited the release profile of *VEGF*. Release of *VEGF* at 1% and 2% O_2 was significantly higher than at 20% or when the inhibitor was used for all time points ($p < 0.01$). Our studies are in agreement with previous studies that have shown that *VEGF* is HIF-1 regulated.[22,26,27,45-48] Our *in vitro* analysis does not include studies looking at the role of HIF-1 in vascularizing bone, but this is a critical process that would need to occur *in vivo*. Blocking vascular growth and maturation will lead to formation of thin, weak bone and this has been demonstrated by previous studies.[24,25] Bone formation *in vivo* requires a coupling of osteogenesis and angiogenesis, making it difficult to evaluate the impact of HIF-1 on each process individually.

Finally, the timing of hypoxic exposure to cells plays a role in this process. A recent study showed the impact of conditioning human MSCs in 2% O_2 before osteogenic differentiation in such an environment.[39] The inhibitory effect of low O_2 on osteogenic differentiation (relative to culture in 20% O_2) was mitigated when the cells were conditioned to this environment before differentiation.

Our results indicate that low O_2 culture reduces osteogenic differentiation of ADSCs compared with atmospheric conditions in a HIF-1-independent manner. However, differentiation will never occur in atmospheric conditions if this event is to take place *in vivo*. Efforts to accelerate bone formation at CSD sites could potentially look at HIF-1 as a therapeutic target, but for modification of processes other than osteogenic differentiation of ADSCs. There are numerous strategies to track the HIF-1 activity at the cellular level.[49,50] These systems show how the cells respond to their local O_2 environment and can guide future work that targets HIF-1. In general, the HIF-1 activity should be beneficial for repair of CSDs, but this effect is not necessarily observed for all processes involved in bone formation.

Acknowledgment

Disclosure Statement

No competing financial interests exist.

References

1. Dupont, K.M., Sharma, K., Stevens, H.Y., Boerckel, J.D., García, A.J., and Guldberg, R.E. Human stem cell delivery for treatment of large segmental bone defects. Proc Natl Acad Sci U S A **107,** 3305, 2010.
2. Chaikof, E.L., Matthew, H., Kohn, J., Mikos, A.G., Prestwich, G.D., and Yip, C.M. Biomaterials and scaffolds in reparative medicine. Ann N Y Acad Sci **961,** 96, 2002.
3. Gamie, Z., Tran, G.T., Vyzas, G., Korres, N., Heliotis, M., Mantalaris, A., and Tsiridis, E. Stem cells combined with bone graft substitutes in skeletal tissue engineering. Expert Opin Biol Ther **12,** 713, 2012.
4. Chimutengwende-Gordon, M., and Khan, W.S. Advances in the use of stem cells and tissue engineering applications in bone repair. Curr Stem Cell Res Ther **7,** 122, 2012.
5. Zuk, P.A., Zhu, M., Ashjian, P., De Ugarte, D.A., Huang, J.I., Mizuno, H., Alfonso, Z.C., Fraser, J.K., Benhaim, P., and Hedrick, M.H. Human adipose tissue is a source of multipotent stem cells. Mol Biol Cell **13,** 4279, 2002.
6. Gimble, J., and Guilak, F. Adipose-derived adult stem cells: isolation, characterization, and differentiation potential. Cytotherapy **5,** 362, 2003.
7. Katz, A.J., Tholpady, A., Tholpady, S.S., Shang, H., and Ogle, R.C. Cell surface and transcriptional characterization of human adipose-derived adherent stromal (hADAS) cells. Stem Cells **23,** 412, 2005.
8. Schmitz, J.P., and Hollinger, J.O. The critical size defect as an experimental model for craniomandibulofacial nonunions. Clin Orthop Relat Res **205,** 299, 1986.
9. Rodriguez-Merchan, E.C., and Forriol, F. Nonunion: general principles and experimental data. Clin Orthop Relat Res **419,** 4, 2004.
10. Heppenstall, R.B., Grislis, G., and Hunt, T.K. Tissue gas tensions and oxygen consumption in healing bone defects. Clin Orthop Relat Res **106,** 357, 1975.
11. Kneser, U., Schaefer, D.J., Polykandriotis, E., and Horch, R.E. Tissue engineering of bone: the reconstructive surgeon's point of view. J Cell Mol Med **10,** 7, 2006.
12. Simon, M.C., and Keith, B. The role of oxygen availability in embryonic development and stem cell function. Nat Rev Mol Cell Biol **9,** 285, 2008.
13. Mohyeldin, A., Garzón-Muvdi, T., and Quiñones-Hinojosa, A. Oxygen in stem cell biology: a critical component of the stem cell niche. Cell Stem Cell **7,** 150, 2010.
14. Watt, F.M., and Hogan, B.L.M. Out of Eden: stem cells and their niches. Science **287,** 1427, 2000.
15. Das, R., Jahr, H., van Osch, G.J., and Farrell, E. The role of hypoxia in bone marrow-derived mesenchymal stem cells: considerations for regenerative medicine approaches. Tissue Eng **16,** 159, 2010.
16. Semenza, G.L. Expression of hypoxia-inducible factor 1: mechanisms and consequences. Biochem Pharmacol **59,** 47, 2000.
17. Semenza, G. Signal transduction to hypoxia-inducible factor 1. Biochem Pharmacol **64,** 993, 2002.
18. Ma, T., Grayson, W.L., Fröhlich, M., and Vunjak-Novakovic, G. Hypoxia and stem cell-based engineering of mesenchymal tissues. Biotechnol Prog **25,** 32, 2009.
19. Dunwoodie, S.L. The role of hypoxia in development of the mammalian embryo. Dev Cell **17,** 755, 2009.
20. Provot, S., and Schipani, E. Fetal growth plate: a developmental model of cellular adaptation to hypoxia. Ann N Y Acad Sci **1117,** 26, 2007.
21. Wan, C., Shao, J., Gilbert, S.R., Riddle, R.C., Long, F., Johnson, R.S., Schipani, E., and Clemens, T.L. Role of HIF-1alpha

in skeletal development. Ann N Y Acad Sci **1192,** 322, 2010.

22. Schipani, E., Maes, C., Carmeliet, G., and Semenza, G.L. Regulation of osteogenesis-angiogenesis coupling by HIFs and VEGF. J Bone Miner Res **24,** 1347, 2009.

23. Tower, D. The osteogenic-angiogenic interface: novel insights into the biology of bone formation and fracture repair. Curr Osteoporos Rep **6,** 67, 2008.

24. Wan, C., Gilbert, S.R., Wang, Y., Cao, X., Shen, X., Ramaswamy, G., Jacobsen, K.A., Alaql, Z.S., Eberhardt, A.W., Gerstenfeld, L.C., Einhorn, T.A., Deng, L., and Clemens, T.L. Activation of the hypoxia-inducible factor-1alpha pathway accelerates bone regeneration. Proc Natl Acad Sci U S A **105,** 686, 2008.

25. Zou, D., Zhang, Z., Ye, D., Tang, A., Deng, L., Han, W., Zhao, J., Wang, S., Zhang, W., Zhu, C., Zhou, J., He, J., Wang, Y., Xu, F., Huang, Y., and Jiang, X. Repair of critical-sized rat calvarial defects using genetically engineered bone marrow-derived mesenchymal stem cells overexpressing hypoxia-inducible factor-1α. Stem Cells **29,** 1380, 2011.

26. Ferrara, N., and Gerber, H.P. The role of vascular endothelial growth factor in angiogenesis. Acta Haematol **106,** 148, 2001.

27. Dai, Y., Xu, M., Wang, Y., Pasha, Z., Li, T., and Ashraf, M. HIF-1alpha induced-VEGF overexpression in bone marrow stem cells protects cardiomyocytes against ischemia. J Mol Cell Cardiol **42,** 1036, 2007.

28. Araldi, E., and Schipani, E. Hypoxia, HIFs and bone development. Bone **47,** 190, 2010.

29. Malladi, P., Xu, Y., Chiou, M., Giaccia, A.J., and Longaker, M.T. Hypoxia inducible factor-1alpha deficiency affects chondrogenesis of adipose-derived adult stromal cells. Tissue Eng **13,** 1159, 2007.

30. Pfander, D., and Gelse, K. Hypoxia and osteoarthritis: how chondrocytes survive hypoxic environments. Curr Opin Rheumatol **19,** 457, 2007.

31. Malladi, P., Xu, Y., Chiou, M., Giaccia, A.J., and Longaker, M.T. Effect of reduced oxygen tension on chondrogenesis and osteogenesis in adipose-derived mesenchymal cells. Am J Physiol Cell Physiol **290,** 1139, 2006.

32. Holzwarth, C., Vaegler, M., Gieseke, F., Pfister, S.M., Handgretinger, R., and Kerst, G., and Müller, I. Low physiologic oxygen tensions reduce proliferation and differentiation of human multipotent mesenchymal stromal cells. BMC Cell Biol **11,** 11, 2010.

33. Fehrer, C., Brunauer, R., Laschober, G., Unterluggauer, H., Reitinger, S., Kloss, F., Gülly, C., Gassner, R., and Lepperdinger, G. Reduced oxygen tension attenuates differentiation capacity of human mesenchymal stem cells and prolongs their lifespan. Aging Cell **6,** 745, 2007.

34. Lennon, D.P., Edmison, J.M., and Caplan, A.I. Cultivation of rat marrow-derived mesenchymal stem cells in reduced oxygen tension: effects on *in vitro* and *in vivo* osteochondrogenesis. J Cell Physiol **187,** 345, 2001.

35. D'Ippolito, G., Diabira, S., Howard, G.A., Roos, B.A., and Schiller, P.C. Low oxygen tension inhibits osteogenic differentiation and enhances stemness of human MIAMI cells. Bone **39,** 513, 2006.

36. Potier, E., Ferreira, E., Andriamanalijaona, R., Pujol, J.P., Oudina, K., Logeart-Avramoglou, D., and Petite, H. Hypoxia affects mesenchymal stromal cell osteogenic differentiation and angiogenic factor expression. Bone **40,** 1078, 2007.

37. Grayson, W.L., Zhao, F., Izadpanah, R., Bunnell, B., and Ma, T. Effects of hypoxia on human mesenchymal stem cell expansion and plasticity in 3D constructs. J Cell Physiol **207,** 331, 2006.

38. Ren, H., Cao, Y., Zhao, Q., Li, J., Zhou, C., Liao, L., Jia, M., Zhao, Q., Cai, H., Han, Z.C., Yang, R., Chen, G., and Zhao, R.C. Proliferation and differentiation of bone marrow stromal cells under hypoxic conditions. Biochem Biophys Res Commun **347,** 12, 2006.

39. Volkmer, E., Kallukalam, B.C., Maertz, J., Otto, S., Drosse, I., Polzer, H., Bocker, W., Stengele, M., Docheva, D., Mutschler, W., and Schieker, M. Hypoxic preconditioning of human mesenchymal stem cells overcomes hypoxia-induced inhibition of osteogenic differentiation. Tissue Eng **16,** 153, 2010.

40. Skiles, M.L., Fancy, R., Topiwala, P., Sahai, S., and Blanchette, J.O. Correlating hypoxia with insulin secretion using a fluorescent hypoxia detection system. J Biomed Mater Res B Appl Biomater **97,** 148, 2011.

41. Lin-Gibson, S., Bencherif, S., Cooper, J.A., Wetzel, S.J., Antonucci, J.M., Vogel, B.M., Horkay, F., and Washburn, N.R. Synthesis and characterization of PEG dimethacrylates and their hydrogels. Biomacromolecules **5,** 1280, 2004.

42. Skiles, M.L., Sahai, S., and Blanchette, J.O. Tracking hypoxic signaling within encapsulated cell aggregates. J Vis Exp **58,** e3521, 2011.

43. Benoit, D.S.W., Durney, A.R., and Anseth, K.S. The effects of heparin-functionalized PEG hydrogels on three-dimensional human mesenchymal stem cell osteogenic differentiation. Biomaterials **28,** 66, 2007.

44. Schipani, E. Hypoxia and HIF-1 alpha in chondrogenesis. Semin Cell Dev Biol **16,** 539, 2005.

45. Brahimi-Horn, M.C., and Pouysségur, J. The hypoxia-inducible factor and tumor progression along the angiogenic pathway. Int Rev Cytol **242,** 157, 2005.

46. Tang, N., Wang, L., Esko, J., Giordano, F.J., Huang, Y., Gerber, H.P., Ferrara, N., and Johnson, R.S. Loss of HIF-1alpha in endothelial cells disrupts a hypoxia-driven VEGF autocrine loop necessary for tumorigenesis. Cancer Cell **6,** 485, 2004.

47. Carroll, V.A., and Ashcroft, M. Role of hypoxia-inducible factor (HIF)-1alpha versus HIF-2alpha in the regulation of HIF target genes in response to hypoxia, insulin-like growth factor-I, or loss of von Hippel-Lindau function: implications for targeting the HIF pathway. Cancer Res **66,** 6264, 2006.

48. Yamazaki, Y., Egawa, K., Nose, K., Kunimoto, S., and Takeuchi, T. HIF-1-dependent VEGF reporter gene assay by a stable transformant of CHO cells. Biol Pharm Bull **26,** 417, 2003.

49. Sahai, S., McFarland, R., Skiles, M.L., Sullivan, D., Williams, A., and Blanchette, J.O. Tracking hypoxic signaling in encapsulated stem cells. Tissue Eng **18,** 557, 2012.

50. Zhou, W., Dosey, T.L., Biechele, T., Moon, R.T., Horwitz, M.S., and Ruohola-Baker, H. Assessment of hypoxia inducible factor levels in cancer cell lines upon hypoxic induction using a novel reporter construct. PLoS One **6,** e27460, 2011.

Address correspondence to:
James O. Blanchette, PhD
Department of Chemical Engineering
University of South Carolina
2C02 Swearingen, 301 Main St.
Columbia, SC 29208

E-mail: blanchej@cec.sc.edu